Article

Chemically-Activated Biochar from *Ricinus communis* L. Cake and Their Potential Applications for the Voltammetric Assessment of Some Relevant Environmental Pollutants

Cristiane Kalinke,[a,b] Paulo R. de Oliveira,[b] Antonio S. Mangrich, [*,c,d]
Luiz H. Marcolino-Junior[b] and Márcio F. Bergamini [*,b]

[a]*Instituto de Química, Universidade Estadual de Campinas (Unicamp), 13083-970 Campinas-SP, Brazil*

[b]*Laboratório de Sensores Eletroquímicos (LabSensE), Departamento de Química,
Universidade Federal do Paraná (UFPR), 81531-980 Curitiba-PR, Brazil*

[c]*Laboratório de Processos e Projetos Ambientais (LabPPAm), Departamento de Química,
Universidade Federal do Paraná (UFPR), 81531-980 Curitiba-PR, Brazil*

[d]*Instituto Nacional de Ciência e Tecnologia de Energia e Ambiente (INCT E&A/CNPq),
Universidade Federal da Bahia (UFBA), 40170-115 Salvador-BA, Brazil*

Biochar is a rich-carbon material highly functionalized, which allows the use as electrodes modifier for preconcentration and voltammetric determination of several species. This work describes a castor cake biochar production and chemical activation with different reaction conditions using HNO_3 and/or H_2O_2. Biochar samples were characterized using scanning electron microscopy, energy dispersive spectroscopy, thermogravimetric analysis, Fourier-transform infrared spectroscopy, Raman and zeta potential. Carbon paste modified electrodes (CPME) have been constructed using different biochar samples to evaluate the adsorptive capacity for the spontaneous preconcentration and voltammetric determination of Pb^{2+}, Cd^{2+}, Cu^{2+} and Ni^{2+} ions, paraquat and methyl parathion pesticides. The activation treatments promoted modifications in the elemental, morphological and structural biochar characteristics. Activated biochar CPMEs showed increase in the current signal around 15 and 2.5 times higher than unmodified and precursor biochar electrode, respectively. N2 sample (HNO_3, 60 °C for 3.0 h) presented the better response signals for all compounds. This was attributed to the more effective surface oxidation, promoting a high porosity, acid character and amount of acid functional groups. Besides that, this greater analytical response allows the CPME-N2 application as a passive sampler for the voltammetric determination of inorganic and organic contaminants for environmental management in aqueous matrices.

Keywords: activated biochar, spontaneous preconcentration, voltammetric detection, inorganic and organic contaminants, environmental remediation

Introduction

Anthropogenic activities produce an elevate amounts of toxic organic and inorganic compounds in the environment, mainly in aqueous effluents.[1] These compounds result in the contamination of other ecosystems and affecting human health.[2] In order to minimize the effect of these contaminants, materials sorbents have been evaluated for sorption and/or retention of inorganic and organic contaminants promoting the removal/immobilization of them from soils and aqueous matrices.[3-5] Biochar is a rich-carbon material highly functionalized obtained by pyrolysis of biomass (vegetable or animal) at controlled temperatures between 300 and 1000 °C, under oxygen limited condition.[6] This material is extensively used for environmental management, such as soil amendment, carbon sequestration and soil/water remediation.[7,8]

Several feedstock can be used for biochar preparation, but industrial and agricultural wastes stand out because they allow the reuse of these materials.[9,10] Castor bean (*Ricinus communis* L.) is a tropical oilseed that has a large oil amount in the seeds.[11] Castor seeds are widely used for the extraction of a non-edible oil rich in ricinoleic acid amount, which makes this oil extraction economically advantageous. The use of castor bean polyurethane is already reported as electrode modifiers for the preconcentration of polar and non-polar species.[12] The production of castor derivates generate a large amount of

*e-mail: mangrich@ufpr.br; bergamini@ufpr.br

waste, which often it does not have an adequate destination. The production of biochar is an excellent alternative for managing wastes since that is simple and low cost process, eco-friendly, sustainable and there are a wide range of applications.[13] In order to improve the performance of the biochar towards preconcentration of organic and inorganic compounds, activation treatments can promote an increase of surface functional groups. For this, different strategies can be employed for biochar activation based on physical or/and chemical process.[14] Chemical activation is based on formation of functional groups at carbonaceous surface by use of chemical agents such as nitric acid,[15] sodium hydroxide,[16] hydrogen peroxide,[17] hydrochloric acid,[18] sulfuric acid,[19] potassium permanganate[20] and others as reported by several authors.[21,22]

Besides of agricultural use of biochar, several papers[23-26] describing its use for construction of voltammetric sensors have been recently reported. These electroanalytical methods are based on spontaneous sorption ability of high functionalized biochar surface for organic and inorganic species. In present paper the preparation and an understanding characterization of biochar chemically activated by HNO_3 and/or H_2O_2 were performed. Different experimental conditions were studied to evaluate the influence of chemical treatment on morphological and structural characteristics of biochar. The activated biochar was used for the construction of carbon paste electrodes and evaluated towards inorganic (Pb^{2+}, Cd^{2+}, Cu^{2+} and Ni^{2+}) and organic species (paraquat and methyl parathion) using a simple, low cost and effective voltammetric approach.

Experimental

Chemical

Solutions were prepared with deionized water by a Millipore Milli-Q® system (Burlington, USA). All the reagents were of analytical grade and were used without further purification. Graphite and mineral oil used for electrodes construction, paraquat and methyl parathion pesticides were acquired from Sigma-Aldrich® (São Paulo, Brazil). Pb^{2+}, Cd^{2+}, Cu^{2+} and Ni^{2+} ions stock solutions were prepared from Merck® (Darmstadt, Germany) standard. Nitric acid and hydrogen peroxide from Neon (Suzano, Brazil) were used as oxidant agents. Hydrochloric acid was obtained from F. Maia® (Belo Horizonte, Brazil). Sodium acetate (J.T. Baker®, Phillipsburg, USA) solution was used as supporting electrolyte, and glacial acetic acid (Isofar®, Duque de Caxias, Brazil) was used to pH adjust.

Biochar preparation and characterization

The preparation of precursor biochar sample was carried out with castor cake biomass obtained from tailings industries in the production of vegetable oil, and which is already used in the biochar production.[27] For this, biomass was macerated using a ball mill and particle size was homogenized with granulometry between 40 and 80 mesh. The samples were submitted to the pyrolysis process under controlled conditions, which were: residence time of 60 min, heating rate of 5 °C min⁻¹ and final temperature of 400 °C. These conditions were chosen because they presented satisfactory results for the voltammetric evaluation, using electrodes modified with biochar.[28]

After the pyrolysis step, the precursor biochar sample (BC) was submitted to different surface treatment processes by chemical activation (Table 1), aiming to increase the amount of surface functional groups and consequently the improvement of the adsorptive capacity of the preconcentration. For this, 50 mL of the oxidizing agent solution, HNO_3 and/or H_2O_2, were added to 1.0 g of precursor biochar. The dispersions were placed in a reflux system, under constant stirring, employing different temperature conditions and reflux time.[29-31] The mixture was filtered, washed with distilled water, oven dried at 100 °C for 24 h, and stored for further use as electrode modifier.

Table 1. Treatment conditions adopted to obtain activated biochar samples with HNO_3 and/or H_2O_2

Sample	Oxidant agent	Reflux condition	
		Temperature / °C	time / h
N1	HNO_3 50% (v/v)	60	1.0
N2	HNO_3 50% (v/v)	60	3.0
N3	HNO_3 50% (v/v)	90	1.0
N4	HNO_3 50% (v/v)	90	3.0
N5	HNO_3 75% (v/v)	60	1.0
H1	H_2O_2 35% (v/v)	40	1.0
H2	H_2O_2 35% (v/v)	40	2.0
NH	HNO_3/H_2O_2 1:1 (v/v)	60	1.0

Precursor and activated biochar samples were characterized by structural and morphological techniques: scanning electron microscopy (SEM), energy dispersive spectroscopy (EDS), thermogravimetric analysis (TGA), Fourier-transform infrared spectroscopy (FTIR), estimation of the number of acid groups by Boehm titration method, Raman spectroscopy and zeta potential (ZP).

SEM images were obtained using a JEOL® (Tokyo, Japan) JSM-6360LV scanning microscope. Semi-quantitative

elemental composition of samples was estimated by EDS analyses using a Thermo model 200 spectroscope (Abingdon, England) with a resolution of 131 eV coupled to the scanning microscope. TGA was conducted in a Netzsch® (Selb, Germany) STA 449F3 thermal analyzer with nitrogen atmosphere (gas flow of 100 mL min⁻¹). Approximately 10 mg of samples were used. The heating rate of 5.0 °C min⁻¹, until 1000 °C was performed. For FTIR measurements 1.0% (m/m) of each biochar sample was homogenized with potassium bromide (KBr) and pressed to obtain a pellet. The pellets were analyzed in a BOMEM® (Quebec, Canada) MB100 spectrophotometer, in the region from 4000 to 400 cm⁻¹, for obtaining information about the functional groups present on the biochar surface. Raman spectroscopy analyses were also carried out using a Witec® (Ulm, Germany) Alpha 300R Raman microscope equipped with a 532 nm laser with a power of 1.5 mW. The acid groups estimation was performed by potentiometric titrations using the method proposed by Boehm.[32] Total acids groups (carboxylic, phenolic and lactonic) were quantified through retro-titration procedure using NaOH to neutralize the acid groups. Initially, 50 mg of biochar were solubilized in 5.0 mL of standardized base (0.10 mol L⁻¹ NaOH). The mixture was kept under constant stirring for 24 h and then filtered. To the filtrate was added an excess of 0.10 mol L⁻¹ HCl (10 mL). Titration was performed using 0.10 mol L⁻¹ NaOH as titrant solution and using a Metrohm® (Utrecht, Netherlands) Titrino Plus titrator. ZP analysis was performed using biochar samples dried at 105 °C for 24 h. A portion of 5.0 mg of each sample was shaken in 50 mL of 0.01 mol L⁻¹ KCl solution, using a shaking incubator at 150 rpm, for 24 h. Solutions of 0.01 mol L⁻¹ HCl and NaOH were added every 200 s to vary the pH values between 3.0 and 8.0. Analyses were performed in a Microtrac Stabino® (Montgomeryville, USA) Particle Charge Mapping titrator.

Electrodes construction

Biochar samples were used for preparation of carbon paste modified electrodes (CPME) aiming to investigate their preconcentration capacity of different electroactive species. For this, electrodes were manufactured using 25% (m/m) mineral oil, 60% (m/m) powder graphite and 15% (m/m) biochar (activated and pristine). Unmodified electrodes (CPE) were also prepared in a proportion of 25 and 75% (m/m) of mineral oil and graphite, respectively. The components were manually homogenized, and the paste formed was compacted in an electrode plastic support of 3.0 mm in diameter and using a copper rod as electrical contact (Figure S1, Supplementary Information (SI) section).

Voltammetric procedures

Differential pulse voltammetry (DPV) measurements were performed using a Metrohm® Autolab potentiostat/galvanostat, managed by NOVA 1.10.5 software, and a conventional electrochemical cell composed of three electrodes. Auxiliary electrode of platinum and Ag|AgCl in 3.0 mol L⁻¹ KCl as reference electrode were used. CPE and CPME with precursor and activated biochar were used as work electrodes. Initially, measurements were carried out to evaluate the potentiality of the proposed electrodes to preconcentrate different inorganic and organic species, being these Pb^{2+}, Cd^{2+}, Cu^{2+} and Ni^{2+} ions, and paraquat (PQ) and methyl parathion (MP) pesticides. The experimental procedures were similar for inorganic (Figure 1a) and organic compounds (Figure 1b), according to methodologies optimized and described in previous studies.[24,28,33,34] For all methodologies, procedures with three steps were used.
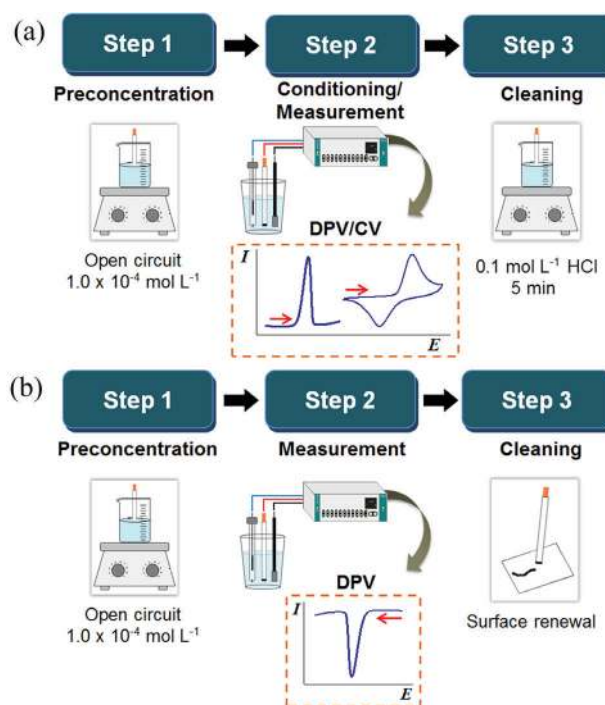

Figure 1. Voltammetric procedures adopted for inorganic (a) and organic compounds (b).

Step 1: preconcentration step

At first, a spontaneous preconcentration step was performed in open circuit potential condition for each individual specie, in 0.10 mol L⁻¹ sodium acetate solution, under constant stirring for 5.0 min. Preconcentration solution with adjusted pH value of 5.0 was used for metallic ions and pesticides.

Step 2: conditioning and measurement steps

After preconcentration step, electrodes were introduced in the electrochemical cell, and different procedures were used to evaluated species.

Step 2a: Pb^{2+}, Cd^{2+} and Cu^{2+}

An additional step was performed to promote the reduction of these ions preconcentrate on surface electrode, applying a potential of −1.0 V during 120 s. Then, DPV measurements were performed aiming the monitoring of metallic ions oxidation, from −1.0 to −0.20 V for Pb^{2+}, from −0.30 to 0.30 V for Cd^{2+} and from −1.1 to −0.50 V for Cu^{2+}, following the conditions: pulse amplitude of 100 mV, pulse time of 25 ms and scan rate of 50 mV s^{-1}.

Step 2b: Ni^{2+}

Detection of Ni^{2+} was performed by the monitoring of Ni^{2+}/Ni^{3+} redox reaction. At first, a conditioning step was performed to promote the oxidation of Ni^{2+} ions preconcentrate on electrode, applying a potential of 0.70 V during 90 s. Cyclic voltammetry measurements were performed in 0.01 mol L^{-1} KOH solution, from 0.30 to 0.70 V, with scan rate of 50 mV s^{-1}.

Step 2c: PQ and MP

Pesticides were detected using the direct reduction by DPV, from −0.90 to −0.10 V for PQ and −1.1 to 0.00 V for MP. Measurements were conducted with following instrumental parameters: pulse amplitude of 25 mV, pulse time of 25 ms and scan rate of 50 mV s^{-1}.

Step 3: cleaning step

The last step performed was the electrode cleaning. For metallic ions, the electrode was put in 0.10 mol L^{-1} HCl solution, under stirring for 5.0 min. For pesticides, the electrode surface was renewed by paper polishing.

Results and Discussion

Scanning electron microscopy and energy dispersive spectroscopy characterizations

Representative SEM images were obtained with 2000 times magnification to evaluate the morphological characteristics of the biochar samples before and after chemical treatment (Figure 2). Some morphological variations between the activated biochar samples were observed. Samples treated with HNO₃ (N1-N5, Figures 2a-2e) exhibited more significant morphological alteration in comparison to biochar pristine (Figure S2, SI section) or treated with H₂O₂. These results can be explained

since that HNO_3 is a more effective oxidant when compared to H_2O_2 and promotes greater alteration of biochar surface. No significant alteration of morphology was observed for biochar treated with H_2O_2 (H1 and H2, Figures 2g-2h). In addition, it can be noted that the NH sample (Figure 2f) treated with a mixture of HNO_3 and H_2O_2 also did not show significant morphological differences, compared to HNO_3 treated samples. Stavropoulos *et al.*[35] evaluated the influence of HNO_3 treatment on activated carbonaceous surface structures and described that chemical treatment had erosive effects on biochar structure. Other authors[20,29] also suggest that these effects could be related to the introduction of functional groups in biochar surface pores. In this sense, porosity and surface area of precursor and N2 activated biochar samples were studied by Brunauer-Emmett-Teller (BET) method in comparison to precursor biochar, in a previous work.[33] It was observed the increase of surface area and a slight increase in volume and diameter of mesopores after activated treatment. Thus, this behavior can be explained by the opening of pores and/or of microchannels structures by the chemical treatment, and the generation of functional groups in the biochar.

Figure 3 shows EDS spectra obtained for the precursor biochar sample in the range of 0.10 to 2.0 keV and for the chemically activated biochar samples between 0.10 and 2.0 keV. EDS spectra of precursor biochar sample (Figure 3a) shows peaks denoting the existence of characteristic elements of this carbonaceous material. The process of obtaining the biochar (pyrolysis) promotes the incomplete combustion of the biomass, thereby some compounds can be formed and others degraded.[27] Thus, both compounds and their content in the biochar can be varied according to the biomass used and the pyrolysis conditions.[8] Pyrolyzed material presented a significant carbon content, and a decrease in oxygen content, as compared to castor cake biomass.[28] Parallel to this, an increase in nitrogen content was observed and can be explained by its incorporation into structures of the material that is heat resistant and non-volatile.[36,37] Mineral compounds, such as magnesium, silicon, sulfur, potassium and calcium, are also commonly found in the product of pyrolysis, and are derived from the raw material used.[1] The presence of the peak relative to aluminum comes from the sample holder used for measurements.

EDS spectra for activated biochar samples (Figure 3b) peaks (normalized) of carbon, oxygen, nitrogen, aluminum and silicon were observed. It is possible that other elements previously observed for the precursor sample may have been removed by the action of surface chemical treatments. Some authors suggest that HNO_3 can promote the release of ions present in biochar. The H⁺ ions are able to displace
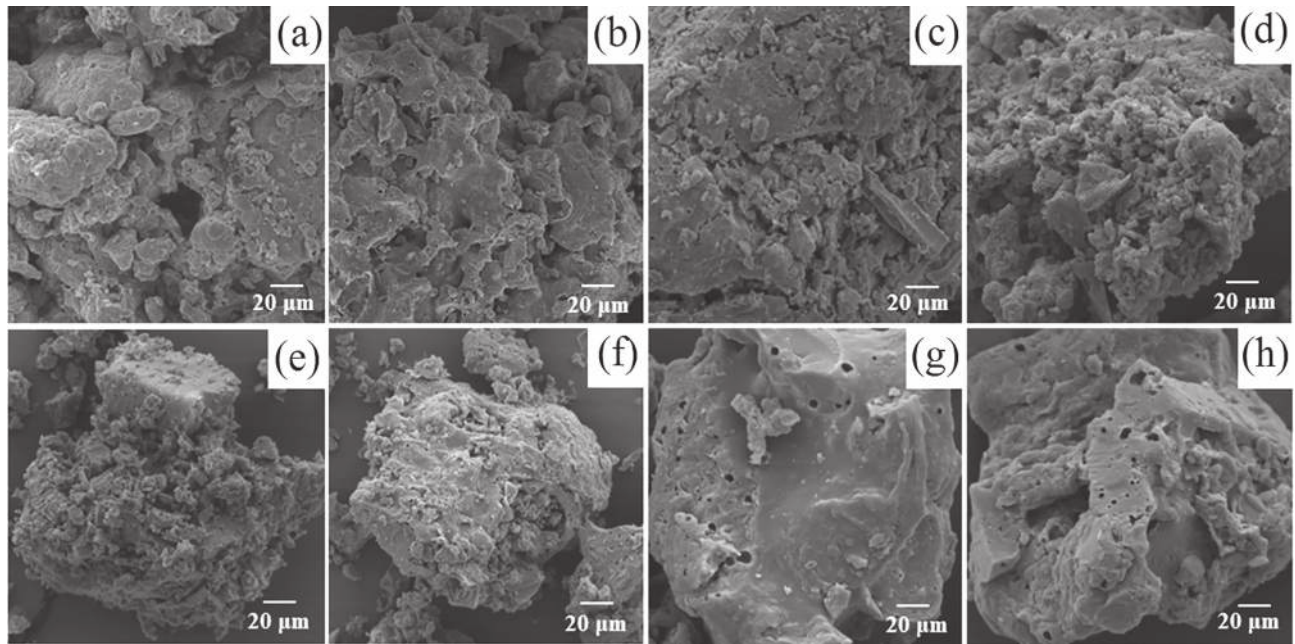
Figure 2. SEM images obtained with 2000 times magnification for activated biochar samples: (a) N1; (b) N2; (c) N3; (d) N4; (e) N5; (f) NH; (g) H1 and (h) H2.
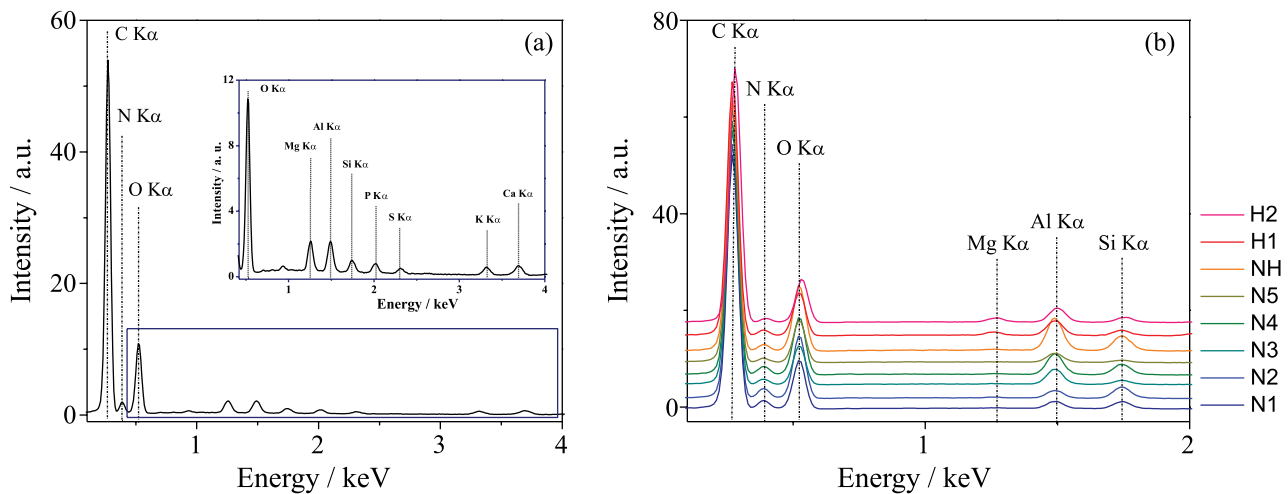

Figure 3. EDS spectra obtained for precursor (a) and activated biochar samples (b).

cations and/or solubilize compounds that are originally present on the biochar surface.[38]

Analyzing the semi-quantitative composition obtained by EDS analyses it was observed variations in the chemical composition after the activation process. Among these, the decrease of the carbon content of the activated samples in comparison to the precursor biochar, which may have been caused by the mineralization of the carbonaceous matrix.[39] However, the samples submitted to H_2O_2 treatment showed an increase in carbon content. The increase in carbon content may be associated with the organic matter remaining in the biochar samples after activation.[20] Another variation was the increase of the oxygen contents observed for all activated biochar samples. Nitrate ions in acid treatment are good

oxidizing agents and promote the oxidation of the biochar surface, leading to the hydroxylic and carboxylic groups formation, which increases the oxygen content. However, the increase of the nitrogen content can be related to the formation of nitro groups, formed by the oxidation of amine groups, or to the adsorption of nitrate ions on the surface of the materials for the treatments with HNO_3.[35] It should be noted that the sample N2 (treated with HNO_3, during 3.0 h at 60 °C) presented the highest elemental variations. For samples H1 and H2, treated with H_2O_2, changes in elemental composition were not significant, which agrees with reports in the literature,[29] and this can be related to the fact that this treatment is less aggressive compared to HNO_3.

Thermogravimetric analysis

In order to obtain information about the biochar thermal behavior before and after activation treatments, TGA analyses were performed providing results based on mass variation of the samples (Figure S3, SI section). For castor cake biomass sample (not pyrolyzed), two thermal processes were observed. The first weight loss of 48.5% at temperature of 310 °C was attributed to hemicellulose degradation. Between 200 and 300 °C the decomposition of hydroxyls and carboxylic groups also can be verified.[8] Up to 400 °C the decomposition of carbohydrates and/or aliphatic compounds occurs.[40] The second process was observed at 477 °C with a weight loss of 34.4%, from cellulosic and aromatic compounds decomposition. Above 600 °C weight losses can be correlated to recalcitrant structures thermally.[41] In addition, the loss of water remaining in the carbonaceous material can be observed from 105 to 200 °C.

Table 2 shows that for both pristine and activated biochar samples only one thermal process related to cellulosic compounds degradation was observed. Lignin degradation occurs slowly to a temperature of 900 °C. For precursor biochar sample it was observed a weight loss of 69.4% at 417 °C. After, the chemical treatment samples have presented an increase in the weight loss compared to this sample. Some authors[42,43] suggest that these weight losses can be mainly associated with the decomposition of carboxylic acid groups (–COOH) and other oxygen groups present in activated samples. This means that the chemical treatments influence in the biochar decomposition. In addition, a displacement in the thermal processes to higher temperatures was observed for the activated samples compared to the BC sample. Samples treated with H_2O_2 presented a lower variation in relation to this thermal process wherein was registered at 440 and 439 °C, with weight losses of 83.0 and 79.3% for samples H1 (refluxing time = 1.0 h) and H2 (refluxing time of 2.0 h), respectively. On the other hand, samples treated with HNO_3 showed a higher displacement of the peaks for this process, registered above 490 °C and with weight losses between 86 and 92%. Inyang *et al.*[44] also obtained materials with greater thermal stability after hickory and sugarcane bagasse biochar activation treatments. The authors recorded displacements in weight loss peaks between 350 and 500 °C with a weight loss of 70 to 80%. Thus, the results obtained may indicate the increase of more difficult structures to be degraded, i.e., more recalcitrant materials after biochar activation treatments.

pH and electrical conductivity (EC)

Results obtained by pH and EC measurements are presented in Table 2. All biochar samples presented an acidic character. Precursor biochar presented a pH of 6.0 and a decrease was observed for activated samples. After activation treatment oxygenated functional groups (e.g., carboxylic acid) are yield on the surface biochar causing the decrease in pH values. Considering that HNO_3 is a stronger oxidant agent when compared to H_2O_2 these results are expected. The N2 sample treated with HNO_3 at 60 °C for 3.0 h has shown the lowest pH value. In addition, this sample also presented a higher EC in comparison to the other activated samples. This behavior can be related to the more functional groups present in surface of this sample. Estupiñan *et al.*[29] showed that coconut shell

Table 2. Characterization responses analyses obtained for precursor and activated biochar samples

Sample	pH	EC / (μS cm⁻¹)	ZP	TGA/DTG		Raman	Boehm titration
			IEP	T / °C	Weight loss / %	I_D/I_G	Total acid groups / (mEq g⁻¹)
BC	6.00 ± 0.20	35.0 ± 1.10	7.31	417	69.4	1.05	5.00 ± 0.29[a]
N1	5.30 ± 0.07	27.5 ± 0.21	5.61	498	89.0	1.20	6.60 ± 0.12
N2	5.10 ± 0.10	30.3 ± 0.14	4.98	495	86.0	1.30	7.90 ± 0.16[a]
N3	5.50 ± 0.07	20.6 ± 0.21	5.72	498	88.3	1.16	5.80 ± 0.18
N4	5.40 ± 0.04	22.9 ± 0.14	5.56	494	88.9	1.11	5.97 ± 0.07
N5	5.50 ± 0.06	14.9 ± 0.07	5.27	490	92.3	1.14	5.60 ± 0.16
NH	5.30 ± 0.10	18.8 ± 0.28	5.41	490	89.8	1.24	7.30 ± 0.05
H1	5.50 ± 0.04	10.2 ± 0.14	6.08	440	83.0	1.14	5.31 ± 0.07
H2	5.60 ± 0.02	13.9 ± 0.07	6.44	439	79.3	1.12	5.30 ± 0.18

[a]Total acid groups values reported in a previous work.[34] EC: electrical conductivity; ZP: zeta potential; TGA/DTG: thermogravimetric analysis/derivative thermogravimetry; IEP: isoelectric point; T: temperature; I_D/I_G: ratio between the intensities of bands D and G; BC: precursor biochar sample; N1-N5: samples treated with HNO_3; NH: sample treated with a mixture of HNO_3 and H_2O_2; H1-H2: samples treated with H_2O_2.

activated biochar samples showed a high increase of acidity for HNO_3 than H_2O_2 treated samples, compared to precursor material. These results were correlated with the increase of oxygen functional groups, following the order: $HNO_3 > H_2O_2 >$ precursor.

In the present paper, precursor material (BC) presented the highest EC in comparison to the all activated materials. This can be explained because of its higher amount of minerals, such as silicates, carbonates and phosphates, as observed by EDS analysis. For BC sample, a high EC can affect the adsorption efficiency by the competition of the substance of interest with these minerals adsorbed superficially, as also reported by other authors.[45,46] On the other hand, the samples submitted to the activation treatments showed a decrease of EC, as expected. In this case, samples treated with H_2O_2 showed the lowest EC values in comparison to samples treated with HNO_3. This last treatment can generate more quantity of functional groups on biochar surface, which can promote the increase of EC due to the presence of these groups.

Zeta potential

ZP is related to particle surface charge and was used to predict the sorption characteristics of biochar samples. The ZP measured for biochar samples varied from 35 to –39 mV in the pH range from 3.0 to 8.0, as presented in Figure 4. The ZP decrease with the pH increase can be due to the adsorption of OH^-, Cl^-, or other anions present in the solution at the biochar surface.[47] For all evaluated samples, ZP values became more negative with pH increase. Precursor biochar showed a ZP less electronegative from 20.4 to –2.28 mV, in comparison to activated biochar samples. The ZP obtained for activated samples (N1, N3, N4, N5, NH, H1 and H2) were nearly similar. Whereas
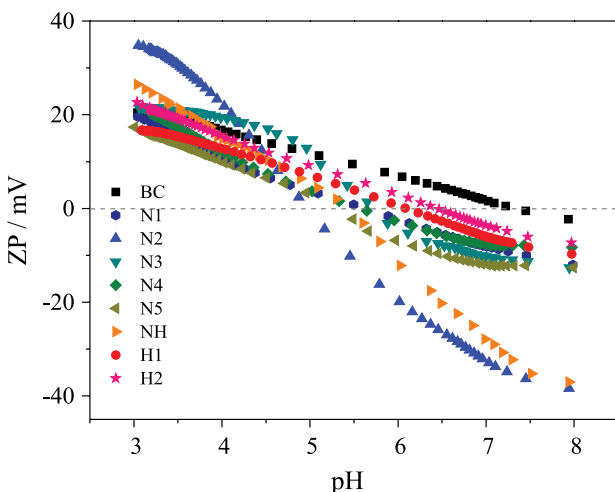

Figure 4. ZP *versus* pH for precursor (BC) and activated biochar samples.

N2 biochar sample presented ZP values significantly more electronegative, from 34.8 to –38.4 mV, compared to all other samples for any pH evaluated. This indicates that N2 sample presents a greater amount of negatively charged on surface than other biochar samples. In addition, particles with higher ZP values (positive or negative) are considered more stable. Typically, to characterize the electrostatic stabilization, minimum ZP values above ± 30 mV are desirable.[48] Based on this, N2 biochar sample can be considered more stable in comparison to the other samples. Similar results were reported by Li *et al.*,[49] biochar samples treated with HNO_3 have showed more negative ZP values when compared to biochar untreated. The authors suggest that this behavior is due to the large amounts of oxygen-containing functional groups as −COOH, −COH and −OH on the activated biochar surface.

The isoelectric points (IEP) of biochar samples were determined from the pH *versus* ZP plot. IEP can be related to pH values at which the ZP is zero and represents the external surface charges of the biochar. The functional groups charge may vary depending on the solution pH, affecting the sorption capacity.[50] However, the higher sorption is observed at values close to the IEP. IEP values from 4.98 to 7.31 were obtained for precursor and activated biochar samples, as presented on Table 2. The results indicated that the biochar surface charges were negative above determined IEP values, as expected. Precursor biochar showed the higher IEP of 7.31, whereas activated biochar samples showed lower values between 4.98 and 6.44. The higher IEP can be an indicative of low amount of surface functional groups. Decrease of IEP values suggests that activation treatments employed were effective to the increase of functional groups at biochar. Thus, this study allowed predicting that the samples with lower IEP value probably will have higher adsorption capacity at this pH, above these values the sorption capacity decreases. The pH of preconcentration solutions was adjusted with these pH values, for spontaneous preconcentration of respective species in biochar samples, following by the voltammetric determinations.

Raman spectroscopy

Raman spectra in the region between 200 and 3000 cm^{-1} were obtained in order to evaluate the degree of disorder of biochar samples (Figure S4, SI section). It was possible to observe the G and D bands in 1570 and 1350 cm^{-1}, respectively. The G band is associated with the stretching of carbon atoms with sp^2 bonds and provides information about the degree of graphitization of the sample. The D band is formed by vibrational forms that become active

when there are defects and functionalities, as –OH and –COOH groups, in the hexagonal planes of these structures.[51,52] Thus, the D and G bands were correlated to obtain the ratio between the bands intensities (I_D/I_G), representative of the biochar defects amount (Table 2). Precursor biochar sample (BC) showed I_D/I_G ratio of 1.05, and for all biochar samples after chemical activation an increase compared with this value was found, related with the increase of surface functional groups. However, N3, N4 and N5 (HNO$_3$ treatment), H1 and H2 samples (H$_2$O$_2$ treatment) exhibited a slight increase of this ratio, from 1.11 to 1.16. N1, N2 and NH samples presented higher values of I_D/I_G of 1.20, 1.30 and 1.24, respectively. In comparison, Inyang *et al.*[44] obtained an increase of I_D/I_G ratio with sugarcane bagasse and hickory chips biochar samples treated with 1.0% (m/m) carbon nanotubes (stirred for 1.0 h). I_D/I_G ratio values from 1.12 to 1.28 and from 1.11 to 1.30 were obtained for the respective samples, before and after activations. Jiang *et al.*[53] also reported a slight increase from 1.05 to 1.18 after the activation of red cedar wood biochar using 0.50 mol L^{-1} HNO$_3$ (overnight, at room temperature). Thus, this increase may mean that the activated material had a higher proportion of surface functional groups, or defects, compared to the precursor biochar sample. In this way, it becomes clear that the introduction of functional groups occurred on the surface of the biochar sample after the activation treatments.

Fourier-transform infrared spectroscopy

FTIR measurements were performed aiming to find information about the functional groups present on the surface of the biochar samples before and after the chemical activation treatments. FTIR spectra (Figure 5) indicate some structural modifications of the biochar after the activation treatments, regarding the spectral distinctions. However, all samples presented bands characteristic of the carbonaceous material. Among the bands observed, around 3400 cm^{-1} corresponding to the stretching of the –OH binding can be highlighted. Vibrations between 3000 and 2800 cm^{-1} can be attributed to C–H stretching, and the spectra of the activated biochar samples showed bands with low intensity in this region.[54] The 1620 cm^{-1} band can be attributed to the C=C stretch of aromatic rings or the C–H deformation. Stretch C=C and folding mode –CH$_2$, related to lignin carbohydrates of the samples, can be characterized by the band at 1430 cm^{-1}. The region between 1400 and 1200 cm^{-1} can be associated with the presence of several clusters, which can lead to overlapping of peaks. However, in relation to the biochar samples, these bands can be attributed to –OH groups of phenols and carboxylic acids. The band at 1030 cm^{-1} can be
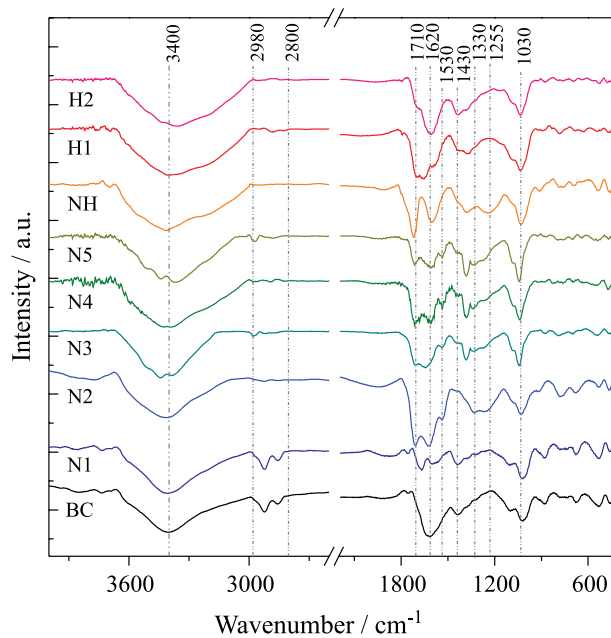

Figure 5. FTIR spectra (KBr) obtained for precursor and activated biochar samples.

attributed to the C–O stretch and to the O–H folding mode of phenols and carboxylic acids.[55] Bands between 1000 and 900 cm^{-1} can be associated with the asymmetric C–O–C stretch, characteristic of cellulosic components (cellulose and lignin) still present in biochar samples.[56] Finally, Si–O bonds can be suggested by the presence of the band at 464 cm^{-1}.[57]

After the activation treatments, other functional groups were generated on the biochar surface. In general, the activated samples presented, among others, bands at 1710 cm^{-1} corresponding to the C=O stretch of carboxylic groups (–COOH). C–O stretch bands and C–O–H asymmetric stretches, both of –COOH, can be attributed to the region around 1250 cm^{-1}.[58] The formation of functional groups after biochar activation can occur in the aliphatic portion of the molecule, breaking the benzyl carbons of C–C bonds or oxidation reactions involving methylene (–CH$_2$).[59] In addition, the presence of nitro groups in the samples can be identified by the bands at 1530 and 1330 cm^{-1} and associated, respectively, to the symmetrical and asymmetrical stretches of the –NO$_2$ group. This suggests that the nitration reaction may occur simultaneously with the oxidation reaction.[55] The introduction of nitro groups superficially adsorbed to the biochar can occur from the nitronium ions that react with the aromatic rings of the biochar structure.[60] In addition, this treatment can release ions from groups existing on the surface of the biochar, i.e., H$^+$ ions of HNO$_3$ can displace and/or solubilize cations that are present in the biochar. This allows more functional groups present in the activated material to be available to interact with other compounds.[42]

Estimate of the amount of acid functional groups

Based on the information obtained by Boehm titrations, the amount of total acid groups (carboxylic, phenolic and lactonic) was estimated in equivalent *per* gram of biochar (mEq g^{-1}) present on the surface of the samples. For this, the samples were neutralized with NaOH, a known excess amount of HCl was added, and potentiometric titrations were performed employing standardized NaOH as titrant solution. Thus, the amounts of total acid groups were obtained by back-titration calculations (Table 2) as compared to the treatment conditions of each activated biochar sample. It can be observed that the biochar samples submitted to the surface activation/functionalization treatments presented an increase of total acidic functional groups in relation to the biochar precursor (BC), which presented a value of 5.0 mmol g^{-1}. The treatments with HNO_3 also allowed the formation of a greater amount of these groups in comparison to the treatments with H_2O_2. These results are consistent with other studies[29,38] and may be related to the treatment conditions that the samples were subjected to, and nitric acid is an oxidant that allows the generation of more acidic oxygenated functional groups. The formation of these groups allows the material to present more active sites to interact with other compounds by different mechanisms of surface interaction.[15] For these treatments, it is observed that in a higher reflux time (3.0 h) the generation of a greater amount of acid groups occurs. This is consistent, since the longer the time of contact with the acid, the greater the formation of these groups.

However, for the treatment employing higher temperature (90 °C) and HNO_3 75% (v/v) no significant variations of total acid groups were observed. This may suggest that the temperature did not present great influences on the biochar functionalization treatments.[13] Thus, there was no need to use reflux temperatures above 60 °C using HNO_3 50% as the oxidizing agent. Based on this information, we highlight the sample N2, obtained in this condition and with reflux time of 3.0 h, which presented the highest amount of formation of acid functional groups, in comparison to the other samples evaluated.

To the titrations of the biochar samples obtained by H_2O_2 treatment, small significant variations were observed for the reaction times of 1.0 and 2.0 h, suggesting that with this oxidizing agent the reflux time did not influence the generation of functional clusters. Thus, it can be assumed that the acid groups estimated for the mixed treatment (HNO_3 + H_2O_2) are mostly due to the use of HNO_3. Thus, it was observed that the chemical treatments performed with HNO_3 showed greater influence on the formation of total acid groups on the surface of the biochar.
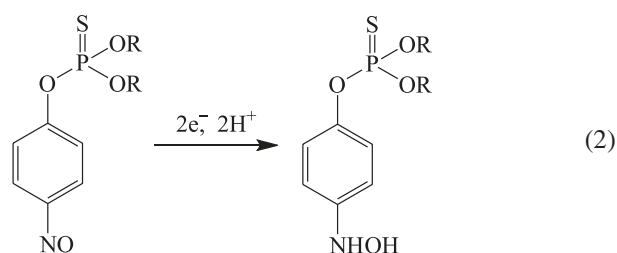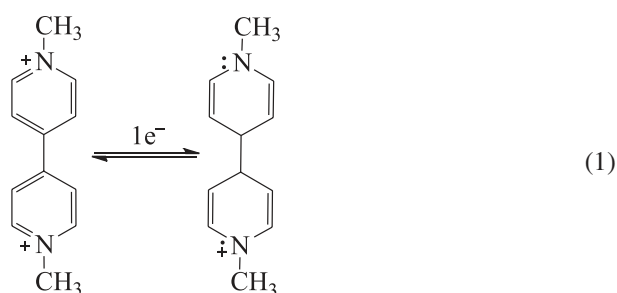
Voltammetric characterization

In order to evaluate the influence of different activation strategies on the biochar samples, they were evaluated as electrode modifiers for preconcentration of different species. Following inorganic and organic species were investigated: Pb^{2+}, Cd^{2+}, Cu^{2+} and Ni^{2+} metallic ions; and pesticides paraquat (PQ) and methyl parathion (MP). Figure S5 (SI section) shows the voltammograms obtained for all evaluated probes. Voltammograms obtained for Pb^{2+} ions (Figure S5a) showed an oxidation peak recorded at −0.61 V for CPE and at −0.55 V for both CPME (*vs.* Ag|AgCl 3.0 mol L^{-1} KCl), which is attributed to the oxidation reaction $Pb^0 \rightarrow Pb^{2+} + 2e^-$. Figure 6a presents the anodic peak current intensity (I_{pa}) obtained by DPV measurements performed after preconcentration of 0.10 mmol L^{-1} Pb^{2+} ions for unmodified (CPE) and biochar precursor (BC) and activated biochar modified electrodes (BC N1, N2, N3, N4, N5, NH, H1 and H2). All modified electrodes (CPME) showed higher response signal compared to CPE, which confirms that the modifications lead to an improvement of the ability of Pb^{2+} preconcentration. In this sense, except the H2 sample (treated with 35% H_2O_2 for 2.0 h), no significant response variations were observed between N1, N3, N4, N5, NH and H1 modified electrodes (Student's statistic *t*-test, 95% confidence). For samples treated with H_2O_2 (H1 and H2), it was observed that the increase in the refluxing time (1.0 and 2.0 h, respectively) caused a slight decrease in the response signal for Pb^{2+} ions. Long time of chemical treatment leads to degradation of H_2O_2 affecting the activation of the biochar surface.[17]

For the electrodes constructed with the samples treated with HNO_3 the increase of the refluxing temperature to 90 °C (N3 and N4 samples) and with concentration of 75% (N5 sample) were not considered determinant parameters, not showing any significant variations in the response signals. However, the reflux time of 3.0 h showed better results than the time of 1.0 h. This is due to the longer contact time of the biochar with the oxidizing agent, which increased the amount of surface functional groups, as evidenced by Boehm titration results.

The best voltammetric responses were obtained using N2 biochar sample as modifier, which was treated with 50% (v/v) HNO_3, at 60 °C for 3.0 h. This sample had the highest surface acid groups estimation, which corroborates the higher amount of oxygen and nitrogen contents estimated by EDS analysis. This resulted in a better voltammetric performance for other evaluated species (inorganic ions and pesticides), as noted in Figure 6b. Cyclic voltammograms performed after nickel preconcentration presented a reversible reaction ($Ni^{2+} \rightleftharpoons Ni^{3+} + 1e^-$), with

anodic and cathodic peaks at 0.59 and 0.49 V, respectively (Figure S5b). DPV voltammograms showed oxidation reactions for Cu^{2+} and Cd^{2+} ions at 0.00 and −0.77 V, respectively (Figures S5c-S5d). Redox reactions for copper and cadmium were similar to proposed for lead, following the oxidation reaction involving 2 electrons: $Cu^0 \rightarrow Cu^{2+} + 2e^-$ and $Cd^0 \rightarrow Cd^{2+} + 2e^-$. Pesticides were evaluated by reduction peaks, both recorded at peak potential of −0.55 V (Figures S5e-S5f). PQ was monitored by the first cathodic peak, attributed to PQ^{2+} reduction to radical cation form ($PQ^{\bullet+}$) (reaction 1).[61] The MP reversible reaction was promoted by the nitro group reduction forming hydroxylamine, as shown in the reaction 2.[62]

$$(1)$$

$$(2)$$

For all evaluated species, the most significant response was registered for CPME-N2 compared to the CPE and modified electrode with biochar precursor (CPME-BC).
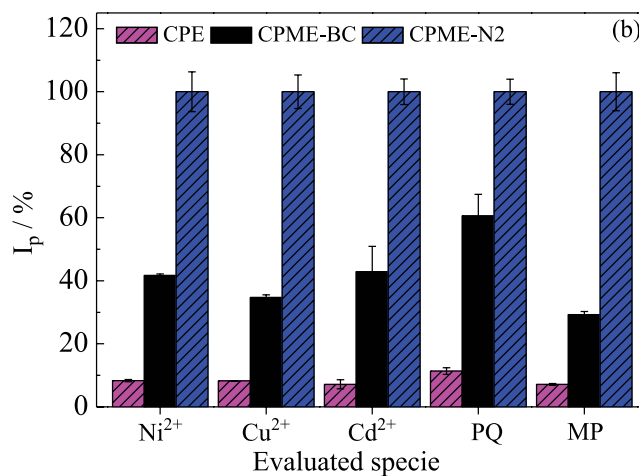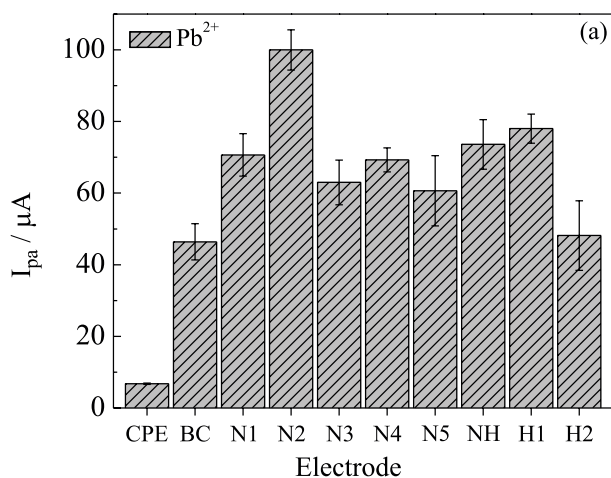
Signals recorded using CPME modified with activated biochar were from 13 to 17 times higher than CPE (unmodified), and between 2 and 3 times higher than CPME-BC. It is important to mention that there are several and different mechanisms proposed to explain the interactions between biochar and inorganic and organic compounds.

For inorganic species, a previous work[28] has revealed that the castor cake biochar interactions occur mainly by a chemisorption mechanism, following the pseudo-second order model. From ZP analysis, it is possible to verify that biochar samples present a negatively charged surface for pH > 4.98. These superficial charges allow biochar interactions with cationic species by electrostatic attraction. In addition, mechanisms relating with ion exchange and/or complexation can also occur promoting better preconcentration of species on electrode surface.[63] The adsorptive capacity of biochar samples for metallic ions preconcentration followed this preference order: $Pb^{2+} > Cd^{2+} > Cu^{2+} > Ni^{2+}$. This behavior can be related to the ionic radius and the hydration energy of the ions. As the evaluated cations have the same oxidation state, the interaction preference increases with the lowest hydrated ionic radius.[64] Pb^{2+} ions present a lower hydrated ionic radius in comparison to the other ions, favoring its mobility to interact with biochar functional groups. For the other ions, the interaction preference can be related to the hydration energy. These results are consistent with other studies reported in the literature,[65,66] in which the lower energy promotes a greater interaction.

In relation to organic species, PQ pesticide is also a cationic compound[67] which may also have favored its better interaction with acid functional groups of the biochar surface, unlike the results observed for MP pesticide, which is a neutral molecule.[68] MP probably binds to the biochar by a mechanism involving hydrogen interactions with the

Figure 6. Correlation of peak current intensity of electrodes evaluated after 0.10 mmol L^{-1} Pb^{2+} ions preconcentration (a); peak current intensities for CPE, CPME-BC and CPME-N2 electrodes after Ni^{2+}, Cu^{2+} and Cd^{2+} ions, and PQ and MP organic compounds preconcentration (b).

MP nitro groups. In addition, π-π-type interactions between the aromatic ring of the pesticide and the carbonaceous part of the biochar may occur, improving the CPME-N2 response signal.[34,69]

Thus, based on results found it was possible to verify that the chemical treatments contributed significantly to improve adsorptive capacity of biochar. This improvement can be associated with a higher quantity of defects and surface acid functional groups in the N2 sample, as evidenced by the characterization analyses. The use of activated biochar enhances the voltammetric response since it allows a high spontaneous preconcentration of organic and inorganic species. Results obtained using CPME-N2 demonstrated greater electroanalytical potential compared to the other biochar samples evaluated, emphasizing this approach for environmental remediation.

Conclusions

Chemical activation treatments of biochar samples have showed different effect on physical and/or chemical properties of the carbonaceous surface. All activated biochar samples showed a greater preconcentration capacity for Pb^{2+}, Cd^{2+}, Cu^{2+} and Ni^{2+} ions, paraquat and methyl parathion pesticides, compared to precursor biochar. CPME modified with biochar sample (N2, treated with 50% HNO_3, 60 °C for 3.0 h) presented best results for both ions and pesticides preconcentration, which improves the voltammetric performance of the sensor. This behavior was associated to the increase of both porosity and acid functional groups of N2 sample. Carbon paste electrode is a feasible, quick, low cost and an easy-construction tool for evaluation of preconcentration features of biochar toward organic and inorganic species. Besides that, there is a possibility to use CPME-N2 as a passive sampler in field for spontaneous preconcentration and effective voltammetric determination of inorganic and organic contaminants.

Supplementary Information

Supplementary information (electrodes construction, thermogravimetric analysis, Raman analysis and voltammetric characterization results) is available free of charge at http://jbcs.sbq.org.br as PDF file.

Acknowledgments

References

1. Noguera-Oviedo, K.; Aga, D. S.; *J. Hazard. Mater.* **2016**, *316*, 242.

2. Matthies, M.; Solomon, K.; Vighi, M.; Gilman, A.; Tarazona, J. V.; *Environ. Sci.: Processes Impacts* **2016**, *18*, 1114.

3. Qian, K.; Kumar, A.; Zhang, H.; Bellmer, D.; Huhnke, R.; *Renewable Sustainable Energy Rev.* **2015**, *42*, 1055.

4. Abdel-Fattah, T. M.; Mahmoud, M. E.; Ahmed, S. B.; Huff, M. D.; Lee, J. W.; Kumar, S.; *J. Ind. Eng. Chem.* **2015**, *22*, 103.

5. Park, S. H.; Cho, H. J.; Ryu, C.; Park, Y.-K.; *J. Ind. Eng. Chem.* **2016**, *36*, 314.

6. Zhang, J.; Liu, J.; Liu, R.; *Bioresour. Technol.* **2015**, *176*, 288.

7. Oliveira, F. R.; Patel, A. K.; Jaisi, D. P.; Adhikari, S.; Lu, H.; Khanal, S. K.; *Bioresour. Technol.* **2017**, *246*, 110.

8. Lehmann, J.; Joseph, S.; *Biochar for Environmental Management: Science and Technology*; Routledge: London, 2012.

9. Tripathi, M.; Sahu, J. N.; Ganesan, P.; *Renewable Sustainable Energy Rev.* **2016**, *55*, 467.

10. Zhang, Y. P.; Adi, V. S. K.; Huang, H.-L.; Lin, H.-P.; Huang, Z.-H.; *J. Ind. Eng. Chem.* **2019**, *76*, 240.

11. Silva, R. V. S.; Casilli, A.; Sampaio, A. L.; Ávila, B. M. F.; Veloso, M. C. C.; Azevedo, D. A.; Romeiro, G. A.; *J. Anal. Appl. Pyrolysis* **2014**, *106*, 152.

12. de Oliveira, J. B.; dos Reis, L. G. T.; Semaan, F. S. In *Polyurethane: Properties, Structure and Application*; Cavaco, L. I.; Melo, J. A., eds.; Nova Science Publishers: New York, 2012, p. 1.

13. Chacón, F. J.; Cayuela, M. L.; Roig, A.; Sánchez-Monedero, M. A.; *Rev. Environ. Sci. Bio/Technol.* **2017**, *16*, 695.

14. Rajapaksha, A. U.; Chen, S. S.; Tsang, D. C.; Zhang, M.; Vithanage, M.; Mandal, S.; Gao, B.; Bolan, N. S.; Ok, Y. S.; *Chemosphere* **2016**, *148*, 276.

15. Jaramillo, J.; Gómez-Serrano, V.; Álvarez, P. M.; *J. Hazard. Mater.* **2009**, *161*, 670.

16. Jung, C.; Boateng, L. K.; Flora, J. R.; Oh, J.; Braswell, M. C.; Son, A.; Yoon, Y.; *Chem. Eng. J.* **2015**, *264*, 1.

17. Xue, Y.; Gao, B.; Yao, Y.; Inyang, M.; Zhang, M.; Zimmerman, A. R.; Ro, K. S.; *Chem. Eng. J.* **2012**, *200*, 673.

18. Arslanoğlu, H.; *J. Hazard. Mater.* **2019**, *374*, 238.

19. Liu, P.; Liu, W.-J.; Jiang, H.; Chen, J.-J.; Li, W.-W.; Yu, H.-Q.; *Bioresour. Technol.* **2012**, *121*, 235.

20. Li, Y.; Shao, J.; Wang, X.; Deng, Y.; Yang, H.; Chen, H.; *Energy Fuels* **2014**, *28*, 5119.

21. Yin, C. Y.; Aroua, M. K.; Daud, W. M. A. W.; *Sep. Purif. Technol.* **2007**, *52*, 403.

22. Cha, J. S.; Park, S. H.; Jung, S.-C.; Ryu, C.; Jeon, J.-K.; Shin, M.-C.; Park, Y.-K.; *J. Ind. Eng. Chem.* **2016**, *40*, 1.

23. Oliveira, P. R.; Lamy-Mendes, A. C.; Gogola, J. L.; Mangrich, A. S.; Marcolino Jr., L. H.; Bergamini, M. F.; *Electrochim. Acta* **2015**, *151*, 525.

24. Kalinke, C.; Mangrich, A. S.; Marcolino-Junior, L. H.; Bergamini, M. F.; *Electroanalysis* **2016**, *28*, 764.

25. Dong, X.; He, L.; Hu, H.; Liu, N.; Gao, S.; Piao, Y.; *Chem. Eng. J.* **2018**, *352*, 371.

26. Ferreira, P. A.; Backes, R.; Martins, C. A.; de Carvalho, C. T.; da Silva, R. A. B.; *Electroanalysis* **2018**, *30*, 2233.

27. Doumer, M. E.; Arízaga, G. G. C.; da Silva, D. A.; Yamamoto, C. I.; Novotny, E. H.; Santos, J. M.; dos Santos, L. O.; Wisniewski, A.; de Andrade, J. B.; Mangrich, A. S.; *J. Anal. Appl. Pyrolysis* **2015**, *113*, 434.

28. Kalinke, C.; Mangrich, A. S.; Marcolino-Junior, L. H.; Bergamini, M. F.; *J. Hazard. Mater.* **2016**, *318*, 526.

29. Estupiñan, P. R.; Giraldo, L.; Moreno, J. C.; *Rev. Colomb. Quim.* **2011**, *40*, 349.

30. Ioannidou, O.; Zabaniotou, A.; *Renewable Sustainable Energy Rev.* **2007**, *11*, 1966.

31. Huff, M. D.; Lee, J. W.; *J. Environ. Manage.* **2016**, *165*, 17.

32. Tsechansky, L.; Graber, E.; *Carbon* **2014**, *66*, 730.

33. Kalinke, C.; Oliveira, P. R.; Oliveira, G. A.; *Anal. Chim. Acta* **2017**, *983*, 103.

34. de Oliveira, P. R.; Kalinke, C.; Gogola, J. L.; Mangrich, A. S.; Junior, L. H. M.; Bergamini, M. F.; *J. Electroanal. Chem.* **2017**, *799*, 602.

35. Stavropoulos, G.; Samaras, P.; Sakellaropoulos, G.; *J. Hazard. Mater.* **2008**, *151*, 414.

36. Gaskin, J.; Steiner, C.; Harris, K.; Das, K.; Bibens, B.; *Trans. Am. Soc. Agric. Eng.* **2008**, *51*, 2061.

37. Al-Wabel, M. I.; Al-Omran, A.; El-Naggar, A. H.; Nadeem, M.; Usman, A. R.; *Bioresour. Technol.* **2013**, *131*, 374.

38. Angelo, L. C.; Mangrich, A. S.; Mantovani, K. M.; dos Santos, S. S.; *J. Soils Sediments* **2014**, *14*, 353.

39. Pradhan, B. K.; Sandle, N.; *Carbon* **1999**, *37*, 1323.

40. Van de Velden, M.; Baeyens, J.; Brems, A.; Janssens, B.; Dewil, R.; *Renewable Energy* **2010**, *35*, 232.

41. Yang, H.; Yan, R.; Chen, H.; Lee, D. H.; Zheng, C.; *Fuel* **2007**, *86*, 1781.

42. El-Hendawy, A.-N. A.; *Carbon* **2003**, *41*, 713.

43. López-Garzón, F. J.; Domingo-García, M.; Pérez-Mendoza, M.; Alvarez, P. M.; Gómez-Serrano, V.; *Langmuir* **2003**, *19*, 2838.

44. Inyang, M.; Gao, B.; Zimmerman, A.; Zhang, M.; Chen, H.; *Chem. Eng. J.* **2014**, *236*, 39.

45. Ng, C.; Losso, J. N.; Marshall, W. E.; Rao, R. M.; *Bioresour. Technol.* **2002**, *84*, 177.

46. Santos, L. B.; Striebeck, M. V.; Crespi, M. S.; Ribeiro, C. A.; de Julio, M.; *J. Therm. Anal. Calorim.* **2015**, *122*, 21.

47. Qian, L.; Chen, B.; *J. Agric. Food Chem.* **2014**, *62*, 373.

48. Honary, S.; Zahir, F.; *Trop. J. Pharm. Res.* **2013**, *12*, 265.

49. Li, H.; Ye, X.; Geng, Z.; Zhou, H.; Guo, X.; Zhang, Y.; Zhao, H.; Wang, G.; *J. Hazard. Mater.* **2016**, *304*, 40.

50. Radovic-Moreno, A. F.; Lu, T. K.; Puscasu, V. A.; Yoon, C. J.; Langer, R.; Farokhzad, O. C.; *ACS Nano* **2012**, *6*, 4279.

51. Robertson, J.; *Mater. Sci. Eng., R* **2002**, *37*, 129.

52. Rhim, Y.-R.; Zhang, D.; Fairbrother, D. H.; Wepasnick, K. A.; Livi, K. J.; Bodnar, R. J.; Nagle, D. C.; *Carbon* **2010**, *48*, 1012.

53. Jiang, J.; Zhang, L.; Wang, X.; Holm, N.; Rajagopalan, K.; Chen, F.; Ma, S.; *Electrochim. Acta* **2013**, *113*, 481.

54. Keiluweit, M.; Nico, P. S.; Johnson, M. G.; Kleber, M.; *Environ. Sci. Technol.* **2010**, *44*, 1247.

55. Mahalakshmy, R.; Indraneel, P.; Viswanathan, B.; *Indian J. Chem.* **2009**, *48*, 352.

56. Ghani, W. A. W. A. K.; Mohd, A.; da Silva, G.; Bachmann, R. T.; Taufiq-Yap, Y. H.; Rashid, U.; Al-Muhtaseb, A. H.; *Ind. Crops Prod.* **2013**, *44*, 18.

57. Tabak, A.; Afsin, B.; Caglar, B.; Koksal, E.; *J. Colloid Interface Sci.* **2007**, *313*, 5.

58. Stainsack, J.; Mangrich, A. S.; Maia, C. M.; Machado, V. G.; dos Santos, J. C.; Nakagaki, S.; *Inorg. Chim. Acta* **2003**, *356*, 243.

59. Chingombe, P.; Saha, B.; Wakeman, R.; *Carbon* **2005**, *43*, 3132.

60. Carey, F. A.; Sundberg, R. J.; *Advanced Organic Chemistry: Structure and Mechanisms*, Part A, 5th ed.; Springer Science & Business Media: New York, USA, 2007.

61. de Oliveira, U. M. F.; Lichtig, J.; Masini, J. C.; *J. Braz. Chem. Soc.* **2004**, *15*, 735.

62. Sanghavi, B. J.; Hirsch, G.; Karna, S. P.; Srivastava, A. K.; *Anal. Chim. Acta* **2012**, *735*, 37.

63. Tan, X.; Liu, Y.; Zeng, G.; Wang, X.; Hu, X.; Gu, Y.; Yang, Z.; *Chemosphere* **2015**, *125*, 70.

64. Braimoh, A.; Vlek, P.; *Land Degrad. Dev.* **2004**, *15*, 65.

65. Güzel, F.; Yakut, H.; Topal, G.; *J. Hazard. Mater.* **2008**, *153*, 1275.

66. Zamzow, M.; Eichbaum, B.; Sandgren, K.; Shanks, D.; *Sep. Sci. Technol.* **1990**, *25*, 1555.

67. Farahi, A.; Achak, M.; El Gaini, L.; El Mhammedi, M. A.; Bakasse, M.; *J. Assoc. Arab Univ. Basic Appl. Sci.* **2016**, *19*, 37.

68. Yao, Y.; Zhang, L.; Xu, J.; Wang, X.; Duan, X.; Wen, Y.; *J. Electroanal. Chem.* **2014**, *713*, 1.

69. Xue, X.; Wei, Q.; Wu, D.; Li, H.; Zhang, Y.; Feng, R.; Du, B.; *Electrochim. Acta* **2014**, *116*, 366.